Noncovalent Porous Materials

DOI: 10.1002/ange.201306785

Permanent Porosity Derived From the Self-Assembly of Highly Luminescent Molecular Zinc Carbonate Nanoclusters**

*Kamil Sokołowski, Wojciech Bury, Iwona Justyniak, David Fairen-Jimenez, Katarzyna Sołtys, Daniel Prochowicz, Sihai Yang, Martin Schröder, and Janusz Lewiński**

Over the past two decades, crystalline microporous materials have attracted major interest, owing to their applications in gas sorption, separation, catalysis, and sensing.[1] Microporous crystalline materials can be constructed from coordinatively or covalently linked building blocks where rigid or semi-rigid molecular scaffolds separate void spaces of different size and geometry. Prominent examples of porous materials showing polymeric structures include zeolites,[2] hybrid metal–organic frameworks (MOFs) or porous coordination polymers (PCPs),[3] covalent organic frameworks (COFs),[4] and H-bonded supramolecular organic frameworks (SOFs).[5] The formation of bonding interactions between building units is an important factor that defines and controls the stability and robustness of these porous polymeric materials. However, discrete molecules may also pack in the solid state to form 3D assemblies that exhibit high permanent porosity.[6] The resulting noncovalent porous materials (NPMs) are distinct from the above polymeric systems, as they are held together by weak noncovalent crystal-packing forces. Modifications of structure by cocrystallization of different building blocks[7] can tune the microcavities in the solid state, and the material can thus conform to the shape or functionality of guest molecules. Moreover, these materials can be highly solubile, an important advantage in their processing to form porous thin films.[7a,8]

NPMs can exhibit extrinsic and/or intrinsic porosity. Intrinsic porosity is associated with the structure of the single-molecule-containing voids, clefts, or cavities, as has been demonstrated for calixarenes,[9] cucurbiturils,[10] cyclodextrins,[11] organic cage compounds,[6,7a,c] or discrete small organic molecules.[12] In contrast, materials with extrinsic porosity are those where individual molecules pack in the solid-state to form structures with empty spaces between the individual molecules. As discrete molecules tend to form close-packed solids with minimal void volume, extrinsic porosity in NPMs remains a rare phenomenon.[12a,13] The rational design and preparation of NPMs showing extrinsic porosity based on molecular metal complexes is highly challenging and few examples have been reported.[14]

We have demonstrated previously that alkylzinc hydroxides RZnOH can be efficiently transformed into multinuclear alkyzinc carbonate nanoclusters[15] or nanomaterials, such as discrete nanoparticulate zinc carbonate aerogels[15] and ZnO nanoparticles.[16] As shown in Scheme 1 a, the reactivity of the RZnOH species can be rationalized in terms of the presence of both a proton-reactive Zn–C bond and CO_2-reactive Zn–OH groups. We argued that introduction of an additional auxiliary ligand L to the RZnOH system, followed by CO_2 fixation, could lead to the formation of novel molecular building blocks for new extrinsic NPMs. Herein, we report such a strategy in which the construction of a nanosized cluster $[Zn_{10}(\mu_6\text{-}CO_3)_4(L)_{12}]$ (**WUT-1**; WUT = Warsaw University of Technology) is achieved by fixation of CO_2 by the tetranuclear hydroxo precursor $[Zn_4(\mu_3\text{-}OH)_2(L)_4(t\text{Bu})_2]$ (**1**;

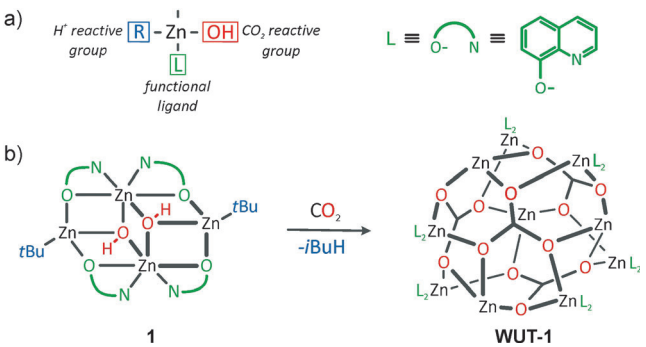

Scheme 1. a) Multifunctional character of R(L)ZnOH moieties. b) The synthesis of **WUT-1** from **1** and CO_2.

[*] Dr. W. Bury, Dr. D. Prochowicz, Prof. J. Lewiński
Faculty of Chemistry, Warsaw University of Technology
Noakowskiego 3, 00-664 Warsaw (Poland)
E-mail: lewin@ch.pw.edu.pl
Homepage: http://lewin.ch.pw.edu.pl
K. Sokołowski, Dr. I. Justyniak, K. Sołtys, Prof. J. Lewiński
Institute of Physical Chemistry, Polish Academy of Sciences
Kasprzaka 44/52, 01-224 Warsaw (Poland)
Dr. D. Fairen-Jimenez
Department of Chemical Engineering & Biotechnology, University of Cambridge
Pembroke Street, Cambridge CB2 3RA (United Kingdom)
Dr. S. Yang, Prof. M. Schröder
School of Chemistry, University of Nottingham, University Park
Nottingham, NG7 2RD (United Kingdom)

[**] The authors acknowledge the Foundation for Polish Science Team Programme co-financed by the EU "European Regional Development Fund" TEAM/2011–7/8 and the National Science Centre (DEC-2011/01/B/ST5/06338) for financial support and the Royal Society (UK) for a University Research Fellowship (D.F.J.). K.S., I.J., and M.S. thank the **N**an**O**technology, **B**iomaterials and a**L**ternative **E**nergy **S**ource for ERA integration (REGPOT-CT-2011-285949-NOBLESSE) Project from the EU. S.Y. gratefully acknowledges the receipt of a Leverhulme Trust Early Career Research Fellowship, and M.S. the receipt of an ERC Advanced Grant and EPSRC Programme Grant. We are grateful to Diamond Light Source for access to the Beamline I11.

Supporting information for this article, including full experimental details for **WUT-1** (experimental procedures, GCMC simulation details, analytical data, X-ray, and spectroscopic data), is available on the WWW under http://dx.doi.org/10.1002/anie.201306785.

L = deprotonated 8-hydroxyquinoline).[17] Packing of single molecules of **WUT-1** leads to the formation of an unprecedented microporous fluorescent NPM within a diamondoid crystal lattice. The permanent porosity in **WUT-1** was confirmed by successful sorption of N_2, H_2, CO_2, and CH_4 at ambient and higher pressures, which can be modeled by grand canonical Monte Carlo (GCMC) simulations.

Reaction of $[Zn_4(\mu_3\text{-}OH)_2(L)_4(t\text{Bu})_2]$ (**1**), a well-characterized complex supported by the luminescent 8-hydroxyquinolinate ligand, in toluene with oxygen-free CO_2 at room temperature resulted in an immediate color change of the solution from yellow to fluorescent green (Scheme 1 b). After 24 h, yellow octahedral crystals of the decanuclear zinc carbonate cluster $[Zn_{10}(\mu_6\text{-}CO_3)_4(L)_{12}]\cdot n(PhMe)$[18] (**WUT-1**) were isolated in 89% yield (Supporting Information, Figure S4). **WUT-1** is stable in the solid state and in solution at ambient temperature under N_2 or dry air. Thermogravimetric analysis (TGA; Figure S10) showed that **WUT-1** quantitatively releases toluene at 90 °C to give desolvated **WUT-1a**.[19] The presence of the carbonate group in **WUT-1** was confirmed by a resonance at 165.3 ppm in the CP-MAS ^{13}C NMR spectrum as well as by a strong band at 1510 cm^{-1}, which is characteristic for a carbonate ligand in the IR spectrum (see the Supporting Information).[15]

The X-ray data for the as-synthesized single crystals of **WUT-1** show residual peaks derived from disordered PhMe molecules (see the Supporting Information). However, this residual amount of solvent can be removed under vacuum (see below) providing desolvated single crystals of **WUT-1a** with the preserved crystal structure (Table S2). The crystal structure of both materials belongs to the cubic space group $Fd\bar{3}$ and contains nanosized (ca. 16 Å) decanuclear core–shell type clusters $[Zn_{10}(\mu_6\text{-}CO_3)_4(L)_{12}]$. The revealed cluster represents a unique example of the zinc carbonate aggregate of fused networks of four- and six-membered heterocyclic rings. The molecular structure of **WUT-1** can be viewed as a tetrahedral zinc carbonate core $[\{Zn(\mu_6\text{-}CO_3)\}_4]$ encapsulated in an octahedral hexazinc quinolinate shell $[\{Zn(L)_2\}_6]$ (Figure 1 a).[29] Each carbonate anion acts as a bridging ligand between six zinc centers, adopting an $\eta^2{:}\eta^2{:}\eta^2{:}\mu_6$-binding (C–O distance = 1.285 Å). Four carbonate ions and four Zn centers occupy alternate locations above the facets of the octahedral $[\{Zn(L)_2\}_6]$ core. Interestingly, every three quinolinate ligands are oriented perpendicularly to the planes of carbonate ions to form four triangular pockets (ca. 3.5 Å in diameter) to give intrinsic pores in the solid state structure of **WUT-1**. A detailed analysis of the crystal structure of **WUT-1** revealed that the spherical nanoclusters self-assemble through $C{-}H_{ar}{\cdots}\pi$ cooperative interactions to produce an extended 3D network with interconnected voids. Based on PLATON calculations, the accessible void fraction in **WUT-1** was estimated to be 0.46 of the unit cell volume, with a solvent-accessible pore volume of 0.50 $cm^3\,g^{-1}$.[20] The geometrical pore-size distribution obtained through molecular simulations for **WUT-1** shows three main pore diameters (Figure S27): 1) ca. 3.5 Å for two types of "ultramicropockets", one surrounded by quinolinate ligands (Figure 1 a, right) and another one on the outer surface of the nodes; 2) cavities of 6.2 Å diameter surrounded by six molecular clusters; 3) the main tetrahedral cavities of 10.4 Å (Figure 1 c). Molecules in **WUT-1** pack to form a diamondoid lattice (Figure 1 b).

WUT-1 was desolvated under a dynamic vacuum (10^{-6} mbar) at 25 °C for 12 h, as confirmed by single-crystal X-ray analysis, ^1H NMR, and TGA measurements (Figures S8 and S10), and does not require any additional activation before gas sorption measurements. At 77 K, the N_2 sorption of the resulting **WUT-1a** exhibits a type I isotherm, which is typical for microporous materials, with a maximum uptake of 308 $cm^3\,g^{-1}$ (39.0 wt%) at standard temperature and pressure (STP) (Figures 2 a and S12). The Brunauer-Emmett-Teller (BET) surface area and the total pore volume for **WUT-1a** calculated from the N_2 adsorption isotherm are 1225 $m^2\,g^{-1}$ and 0.48 $cm^3\,g^{-1}$, respectively. This is the highest value for NPMs based on metal clusters, and is among the highest values for all NPMs (Table S5).[6b,13] For a better analysis of the adsorption data at low pressures, the isotherm was plotted using a semi-logarithmic scale. The isotherm presents a complex shape with an initial step around 3.5 mmol g^{-1} (Figure 2 a, bottom). The presence of steps in the adsorption isotherms is generally explained by the existence of structural changes in flexible materials[21] or by stepwise filling of different pores and adsorption sites.[22]

To investigate the step in the isotherm and to relate it to a potential structural change of **WUT-1a**, we conducted GCMC simulations of N_2 sorption at 77 K following an approach that is routinely applied to studies of flexible

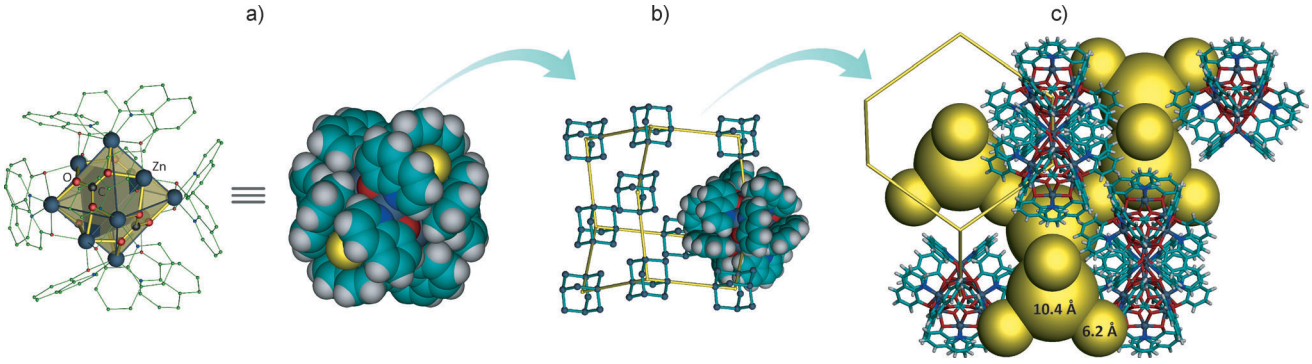

Figure 1. a) Ball and stick (left) and space-filled (right) views of the molecular structure of **WUT-1**. Yellow spheres represent 3.5 Å diameter ultramicropockets resulting from the arrangement of quinolinate ligands. b) The diamondoid lattice of **WUT-1**. c) Projection of the unit cell in **WUT-1** along (110) with yellow spheres representing cavities.

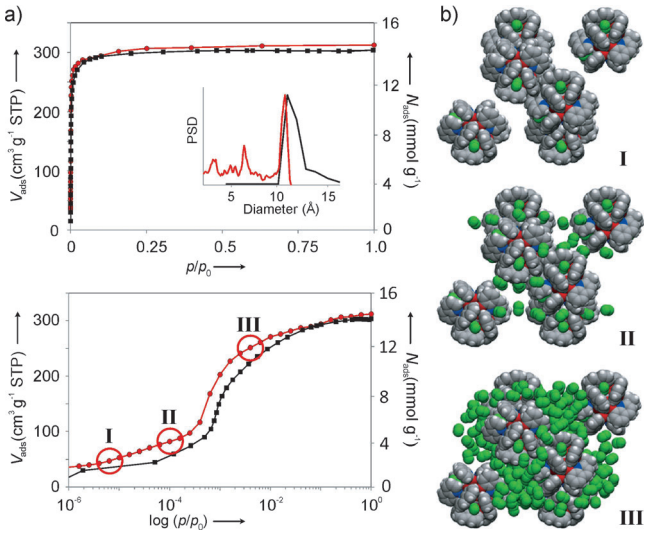

Figure 2. a) Experimental (■) and simulated (●) N_2 isotherms of **WUT-1a** obtained at 77 K using standard (top) and semi-logarithmic scale (bottom). Circled data points indicate the isotherm points for the snapshots. Inset shows the geometrical (——) and DFT (——) pore-size distribution. b) The adsorption mechanism of N_2 on **WUT-1a** at 77 K using snapshots at three different loadings, as indicated on the semi-logarithmic-scaled isotherm.

MOFs.[21,23] In the present case, the simulated isotherm reproduces the experimental shape very well, with a BET area and a total pore volume (1205 $m^2 g^{-1}$ and 0.49 $cm^3 g^{-1}$, respectively) that match the experimental values. The GCMC simulation shows that N_2 molecules first occupy the ultramicropockets formed by three quinolinate ligands, (four ultramicropockets in each cluster) followed by adsorption between clusters, and finally by saturation in the main cavities (Figure 2a, b and Figure S32). The ability of a rigid structural model to predict the experimental gas adsorption isotherm suggests that the existence of steps in the N_2 isotherm is related to the presence of different adsorption sites with strong interactions in **WUT-1a** rather than a framework flexibility phenomenon.[24] This was confirmed by PXRD measurements with increasing CO_2 loadings, which show no major structural changes upon gas loading or desolvation (Figure S5 and Table S3).

Evaluation of the H_2 adsorption in **WUT-1a** at 77 K (Figure 3a and Figure S15) revealed an uptake of 1.0 wt% (116 $cm^3 g^{-1}$ STP, 1.1 bar) and 1.9 wt% (216 $cm^3 g^{-1}$ STP, 20 bar). GCMC simulations match the experimental data and predict a maximum capacity of 2.1 wt% (77 K, 20 bar). Analysis of the isosteric heat of adsorption (Q_{st}) plot shows the presence of two distinct regimes with a very high initial value of 12.2 kJ mol^{-1} (Figures 3d and S18), which gradually decreases to reach 5.7 kJ mol^{-1} at a 3 mmol g^{-1} loading of H_2. The high initial value of Q_{st} can be rationalized in terms of the adsorption of H_2 molecules in ultramicropockets, as confirmed by GCMC simulations (Figure S34). Importantly, high Q_{st} values of up to 15.1 kJ mol^{-1} have been observed in MOFs with coordinatively unsaturated metal sites, whereas values of 3.8–9.5 kJ mol^{-1} are typically reported for MOFs without open metal sites.[1b] Both the significant H_2 capacity and the very high initial Q_{st} make **WUT-1a** an interesting model system for discussing the fundamental phenomena of H_2 adsorption in porous materials.

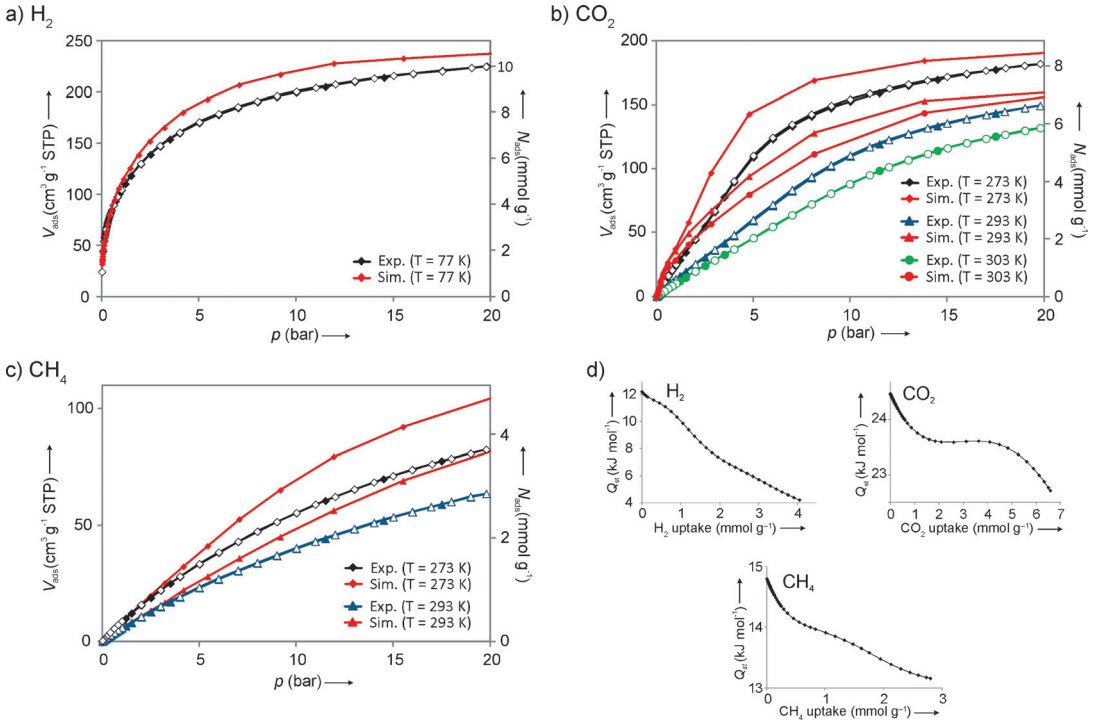

Figure 3. Experimental and simulated data for **WUT-1a**. a) H_2 isotherms at 77 K. (b) CO_2 isotherms at 273, 293, and 303 K. c) CH_4 isotherms at 273 and 293 K. d) Isosteric heat of adsorption plots for H_2, CO_2, and CH_4. Adsorption and desorption branches are shown with closed and open symbols, respectively.

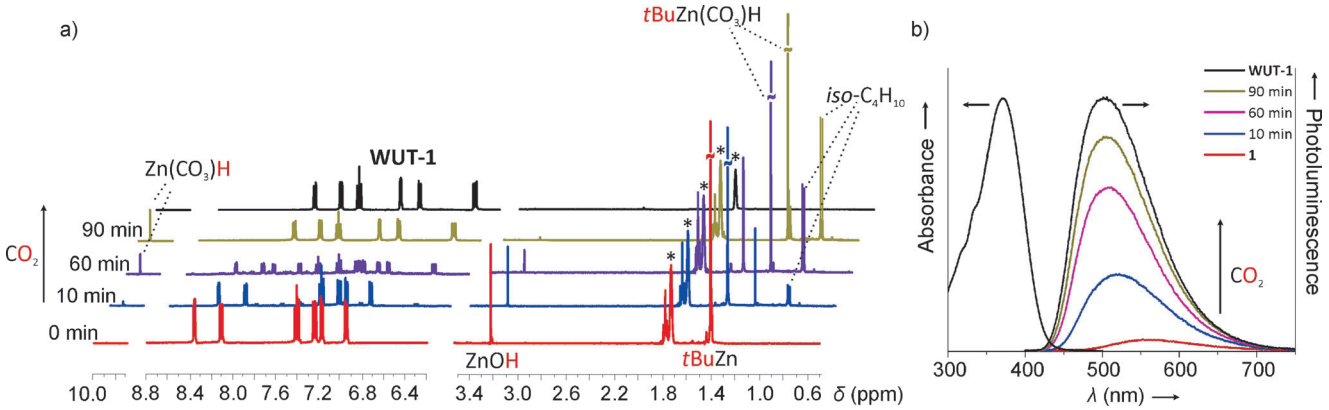

Figure 4. a) ^{1}H NMR spectra for the CO_2 activation by **1** in [D_8]THF. b) Absorbance (max. at 370 nm) and photoluminescence (max. at 480 nm; excitation at 370 nm) spectra of **WUT-1** (——) in THF; color curves indicate changes in photoluminescence spectra during CO_2 fixation.

The adsorption properties of **WUT-1a** are further exemplified by significant CO_2 uptakes (Figures 3b, S19, and S20) at 195 K and 273 K at up to 1 bar, as well as 20 bar at three temperatures (273, 293, and 303 K). The total uptakes for CO_2 at 1 bar (195 K), 1 bar (273 K) and 20 bar (273 K) reached 46.2 wt% (235 $cm^3 g^{-1}$ STP), 4.8 wt% (24.4 $cm^3 g^{-1}$ STP), and 35.3 wt% (182 $cm^3 g^{-1}$ STP), respectively. The Q_{st} plots calculated for CO_2 (Figures 3d and S23) show similar features to the one observed for H_2, with a value of 24.5 kJ mol^{-1} at zero coverage, which gradually decreases to 23.5 kJ mol^{-1} at a 2–3 mmol g^{-1}loading of CO_2. GCMC simulations for CO_2 adsorption on a rigid model slightly surpass the experimental results, and predict capacities of 47 wt% (195 K) and 38 wt% (273 K) (Figures 3b and S35).[25] More in-depth analysis of CO_2 uptake snapshots for different temperatures shows that the ultramicropockets are accessible to the CO_2 molecules. However, this takes place predominately at low temperatures such as 195 K and only to a minor extent at higher temperatures such as 273 K (Figure S36 and S37). Notably, the in situ PXRD data collected for a **WUT-1a** sample at increasing CO_2 loadings (Figure S5 and Table S4) demonstrate that the there is no significant change in the unit cell parameters. This observation further confirms that the origin of the steps observed in the isotherms can be assigned to the stepwise filling mechanism discussed above.

The high porosity in **WUT-1** also enables high methane storage capacity (Figure 3c). At 20 bar, the CH_4 capacity of **WUT-1a** reaches 5.8 wt% (90 $cm^3 g^{-1}$ STP) and 4.5 wt% (70 $cm^3 g^{-1}$ STP) at 273 and 293 K, respectively. Notably, the volumetric uptakes[26] of CH_4 equal 63 g L^{-1} at 273 K and 49 g L^{-1} at 293 K, and are moderate compared with state-of-the-art MOFs such as PCN-14, NOTT-122, and NU-125.[27] However, to our knowledge, these values are the highest reported for NPMs. Importantly, none of the CH_4 isotherms reach saturation at 20 bar, so higher uptakes might be expected at higher pressures. Again, the Q_{st} profile for CH_4 is complex (Figures 3d and S26), with a Q_{st} value of 14.8 kJ mol^{-1} at zero coverage.

To obtain a better understanding of the reaction mechanism of the organozinc precursor **1** with CO_2 and the formation of **WUT-1**, we performed more detailed spectroscopic studies. The in situ ^{1}H NMR spectral analysis in [D_8]THF indicated that the formation of **WUT-1** proceeds through a bicarbonate intermediate and was complete after 3 h (Figure 4a). The gradual disappearance of ZnOH signals (3.22 ppm) and the formation of transient $Zn(HCO_3)$ species (9.90 ppm) with a concomitant formation of isobutane (0.89 ppm) strongly supports the hypothesis of stepwise proton transfer between functional groups in the trifunctional precursor **1**. Additionally, the course of the reaction of **1** with CO_2 was monitored by photoluminescence (PL) spectroscopy. When a toluene solution of **1** in a quartz cuvette was exposed to CO_2, a rapid increase in intensity of the PL band was observed with a gradual shift of the peak maximum from 555 nm (characteristic for **1**) to 480 nm (**WUT-1**) (Figure 4b). This observation is in good agreement with the very high value of the quantum yield (QY) measured for **WUT-1** (QY = 65%), as compared to the parent compound **1** (QY = 5%)[17] and the well-studied complex [$Zn(L)_2$] (QY = 3%).[28]

In conclusion, we have demonstrated a novel synthetic approach to functional materials involving CO_2 fixation by a well-defined organozinc hydroxide precursor. This approach afforded the unique and permanently porous fluorescent NPM **WUT-1** based on discrete zinc carbonate hydroxyquinolinate nanoclusters. **WUT-1** exhibits a noncovalent diamondoid 3D microporous structure with one of the highest BET surface area for NPM materials. The experimental gas adsorption isotherms and GCMC simulations confirm the strong binding of H_2 to **WUT-1** clusters with a heat of adsorption of 12.2 kJ mol^{-1} at zero coverage. This can be rationalized in terms of occupation of the strong binding sites in the ultramicropockets on the surface of **WUT-1**, involving discrete clusters in the first step of H_2 sorption. We believe that the reported synthetic approach utilizing the unique reactivity of well-defined organozinc precursors will provide new perspectives on the preparation of metallosupramolecular architectures with desired functionalities.

Received: August 2, 2013
Revised: September 4, 2013
Published online: October 14, 2013

Keywords: carbon dioxide · chemisorption · hydroxyquinolines · luminescence · zinc hydroxide

[1] a) K. Sumida, D. L. Rogow, J. A. Mason, T. M. McDonald, E. D. Bloch, Z. R. Herm, T.-H. Bae, J. R. Long, *Chem. Rev.* **2012**, *112*, 724 – 781; b) M. P. Suh, H. J. Park, T. K. Prasad, D.-W. Lim, *Chem. Rev.* **2012**, *112*, 782 – 835; c) X. Lin, N. R. Champness, M. Schröder, *Top. Curr. Chem.* **2010**, *293*, 35 – 76; d) J. Lee, O. K. Farha, J. Roberts, K. A. Scheidt, S. T. Nguyen, J. T. Hupp, *Chem. Soc. Rev.* **2009**, *38*, 1450 – 1459.

[2] T. L. M. Maesen, B. Marcus in *Introduction to Zeolite Science and Practice* (Eds.: H. van Bekkum, E. M. Flanigen, P. A. Jacobs, J. C. Jansen), Elsevier, Amsterdam, **2001**, pp. 1 – 9.

[3] *Metal-Organic Frameworks, Design and Application* (Ed.: L. R. MacGillivray), Wiley, Hoboken, **2010**.

[4] X. Feng, X. Dinga, D. Jiang, *Chem. Soc. Rev.* **2012**, *41*, 6010 – 6022.

[5] W. Yang, A. Greenaway, X. Lin, R. Matsuda, A. J. Blake, C. Wilson, W. Lewis, P. Hubberstey, S. Kitagawa, N. R. Champness, M. Schröder, *J. Am. Chem. Soc.* **2010**, *132*, 14457 – 14469.

[6] a) A. I. Cooper, *Angew. Chem.* **2012**, *124*, 8014 – 8016; *Angew. Chem. Int. Ed.* **2012**, *51*, 7892 – 7894; b) M. Mastalerz, *Angew. Chem.* **2012**, *124*, 604 – 606; *Angew. Chem. Int. Ed.* **2012**, *51*, 584 – 586; c) M. Mastalerz, *Chem. Eur. J.* **2012**, *18*, 10082 – 10091; d) J. R. Holst, A. Trewin, A. I. Cooper, *Nat. Chem.* **2010**, *2*, 915 – 920; e) N. B. McKeown, *J. Mater. Chem.* **2010**, *20*, 10588 – 10597.

[7] a) M. W. Schneider, I. M. Oppel, A. Griffin, M. Mastalerz, *Angew. Chem.* **2013**, *125*, 3699 – 3703; *Angew. Chem. Int. Ed.* **2013**, *52*, 3611 – 3615; b) M. W. Schneider, I. M. Oppel, H. Ott, L. G. Lechner, H.-J. S. Hauswald, R. Stoll, M. Mastalerz, *Chem. Eur. J.* **2012**, *18*, 836 – 847; c) J. T. A. Jones, T. Hasell, X. Wu, J. Bacsa, K. E. Jelfs, M. Schmidtmann, S. Y. Chong, D. J. Adams, A. Trewin, F. Schiffmann, F. Cora, B. Slater, A. Steiner, G. M. Day, A. I. Cooper, *Nature* **2011**, *474*, 367 – 371; d) M. Mastalerz, W. Schneider, I. M. Oppel, O. Presly, *Angew. Chem.* **2011**, *123*, 1078 – 1083; *Angew. Chem. Int. Ed.* **2011**, *50*, 1046 – 1051; e) R. Natarajan, G. Magro, L. N. Bridgland, A. Sirikulkajorn, S. Narayanan, L. E. Ryan, M. F. Haddow, A. G. Orpen, J. P. H. Charmant, A. J. Hudson, A. P. Davis, *Angew. Chem.* **2011**, *123*, 11588 – 11592; *Angew. Chem. Int. Ed.* **2011**, *50*, 11386 – 11390.

[8] a) M. Brutschy, M. W. Schneider, M. Mastalerz, S. R. Waldvogel, *Adv. Mater.* **2012**, *24*, 6049 – 6052; b) T. Hasell, H. Zhang, A. I. Cooper, *Adv. Mater.* **2012**, *24*, 5732 – 5737; c) T. Hasell, S. Y. Chong, M. Schmidtmann, D. J. Adams, A. I. Cooper, *Angew. Chem.* **2012**, *124*, 7266 – 7269; *Angew. Chem. Int. Ed.* **2012**, *51*, 7154 – 7157.

[9] a) C. Tedesco, L. Erra, M. Brunelli, V. Cipolletti, C. Gaeta, A. N. Fitch, J. L. Atwood, P. Neri, *Chem. Eur. J.* **2010**, *16*, 2371 – 2374; b) S. J. Dalgarno, P. K. Thallapally, L. J. Barbour, J. L. Atwood, *Chem. Soc. Rev.* **2007**, *36*, 236 – 245.

[10] a) J. Tian, S. Ma, P. K. Thallapally, D. Fowler, B. P. McGrail, J. L. Atwood, *Chem. Commun.* **2011**, *47*, 7626 – 7628; b) H. Kim, Y. Kim, M. Yoon, S. Lim, S. M. Park, G. Seo, K. Kim, *J. Am. Chem. Soc.* **2010**, *132*, 12200 – 12202.

[11] R. A. Smaldone, R. S. Forgan, H. Furukawa, J. J. Gassensmith, A. M. Z. Slawin, O. M. Yaghi, J. F. Stoddart, *Angew. Chem.* **2010**, *122*, 8812 – 8816; *Angew. Chem. Int. Ed.* **2010**, *49*, 8630 – 8634.

[12] a) M. Mastalerz, I. M. Oppel, *Angew. Chem.* **2012**, *124*, 5345 – 5348; *Angew. Chem. Int. Ed.* **2012**, *51*, 5252 – 5255; b) P. Sozzani, S. Bracco, A. Comotti, L. Ferretti, R. Simonutti, *Angew. Chem.* **2005**, *117*, 1850 – 1854; *Angew. Chem. Int. Ed.* **2005**, *44*, 1816 – 1820.

[13] To date there are only few materials exhibiting a successful combination of both types of porosity, including a family of phthalocyanine unsolvated nanoporous crystals (PUNC) and triptycenetrisbenzimidazolone (TTBI) with permanent porosity BET surface areas of 1002 $m^2 g^{-1}$ and 2796 $m^2 g^{-1}$, respectively: see Ref. [12a] and C. G. Bezzu, M. Helliwell, J. E. Warren, D. R. Allan, N. B. McKeown, *Science* **2010**, *327*, 1627 – 1630.

[14] a) P. S. Nugent, V. L. Rhodus, T. Pham, K. Forrest, L. Wojtas, B. Space, M. J. Zaworotko, *J. Am. Chem. Soc.* **2013**, *135*, 10950 – 10953; b) J. Lewiński, T. Kaczorowski, D. Prochowicz, T. Lipińska, I. Justyniak, Z. Kaszkur, J. Lipkowski, *Angew. Chem.* **2010**, *122*, 7189 – 7193; *Angew. Chem. Int. Ed.* **2010**, *49*, 7035 – 7039; c) R. Murugavel, S. Kuppuswamy, N. Gogoi, R. Boomishankar, A. Steiner, *Chem. Eur. J.* **2010**, *16*, 994 – 1009; d) T. Kaczorowski, I. Justyniak, T. Lipińska, J. Lipkowski, J. Lewiński, *J. Am. Chem. Soc.* **2009**, *131*, 5393 – 5395; e) S. A. Dalrymple, G. K. H. Shimizu, *J. Am. Chem. Soc.* **2007**, *129*, 12114 – 12116; f) K. Yamada, S. Yagishita, H. Tanaka, K. Tohyama, K. Adachi, S. Kaizaki, H. Kumagai, K. Inoue, R. Kitaura, H. C. Chang, S. Kitagawa, S. Kawata, *Chem. Eur. J.* **2004**, *10*, 2647 – 2660.

[15] K. Sokołowski, W. Bury, I. Justyniak, A. M. Cieślak, M. Wolska, K. Sołtys, I. Dzięcielewski, J. Lewiński, *Chem. Commun.* **2013**, *49*, 5271 – 5273.

[16] W. Bury, E. Krajewska, M. Dutkiewicz, K. Sokołowski, I. Justyniak, Z. Kaszkur, K. J. Kurzydłowski, T. Płociński, J. Lewiński, *Chem. Commun.* **2011**, *47*, 5467 – 5469.

[17] K. Sokołowski, I. Justyniak, W. Śliwiński, K. Sołtys, A. Tulewicz, A. Kornowicz, R. Moszyński, J. Lipkowski, J. Lewiński, *Chem. Eur. J.* **2012**, *18*, 5637 – 5645.

[18] The analysis of the ^{1}H NMR spectra, TGA profiles, and single crystal X-ray diffraction data suggests the incorporation of 1–2.5 solvent molecules per molecular cluster.

[19] The resulting framework remains thermally stable at least to 125 °C, as indicated by variable-temperature single-crystal X-ray diffraction analysis and gas adsorption measurements (Table S3 and Figure S12 b).

[20] PLATON, A. L. Spek Utrecht Univ., Utrecht, The Netherlands, **2000**.

[21] D. Fairen-Jimenez, S. A. Moggach, M. T. Wharmby, P. A. Wright, S. Parsons, T. Düren, *J. Am. Chem. Soc.* **2011**, *133*, 8900 – 8902.

[22] a) J. Getzschmann, I. Senkovska, D. Wallacher, M. Tovar, D. Fairen-Jimenez, T. Düren, J. M. van Baten, R. Krishna, S. Kaskel, *Microporous Mesoporous Mater.* **2010**, *136*, 50 – 58; b) S. Yang, X. Lin, W. Lewis, M. Suyetin, E. Bichoutskaia, J. E. Parker, C. C. Tang, D. R. Allan, P. J. Rizkallah, P. Hubberstey, N. R. Champness, K. M. Thomas, A. J. Blake, M. Schröder, *Nat. Mater.* **2012**, *11*, 710 – 716.

[23] N. A. Ramsahye, G. Maurin, S. Bourrelly, P. L. Llewellyn, T. Loiseau, C. Serre, G. Ferey, *Chem. Commun.* **2007**, 3261 – 3263.

[24] For many examples of breathing, dynamic, spring-like, sponge-like, or accordion effects in MOFs, see: G. Férey, C. Serre, *Chem. Soc. Rev.* **2009**, *38*, 1380 – 1399.

[25] Small overpredictions are provoked by uncertainties in the Dreiding force field: D. Fairen-Jimenez, R. Galvelis, A. Torrisi, A. D. Gellan, M. T. Wharmby, P. A. Wright, C. Mellot-Draznieks, T. Düren, *Dalton Trans.* **2012**, *41*, 10752 – 10762.

[26] Value estimated for bulk a **WUT-1a** density of 1.098 $g cm^{-3}$.

[27] a) Y. Yan, M. Suyetin, E. Bichoutskaia, A. J. Blake, D. R. Allan, S. A. Barnett, M. Schröder, *Chem. Sci.* **2013**, *4*, 1731 – 1736; b) C. E. Wilmer, O. K. Farha, T. Yildirim, I. Eryazici, V. Krungleviciute, A. A. Sarjeant, R. Q. Snurr, J. T. Hupp, *Energy Environ. Sci.* **2013**, *6*, 1158 – 1163; c) S. Ma, D. Sun, J. M. Simmons, C. D. Collier, D. Yuan, H.-C. Zhou, *J. Am. Chem. Soc.* **2008**, *130*, 1012 – 1016.

[28] S. Li, J. Lu, H. Ma, D. Yan, Z. Li, S. Qin, D. G. Evans, X. Duan, *J. Phys. Chem. C* **2012**, *116*, 12836 – 12843.

[29] CCDC 953686 (**WUT-1**) and 953685 (**WUT-1a**) contain the supplementary crystallographic data for this paper. These data can be obtained free of charge from The Cambridge Crystallographic Data Centre via www.ccdc.cam.ac.uk/data_request/cif.

